ELSEVIER

Contents lists available at ScienceDirect

Journal of Molecular Spectroscopy

journal homepage: www.elsevier.com/locate/yjmsp





Helium nanodroplet isolation spectroscopy in an undergraduate teaching laboratory

Paul L. Raston

Department of Chemistry and Biochemistry, James Madison University, Harrisonburg, VA 22807, USA

ARTICLE INFO

Keywords: Infrared spectroscopy Helium nanodroplets Formic acid Undergraduate research

ABSTRACT

A home-built helium nanodroplet isolation spectrometer has been utilized by undergraduate students in course-based experiments to investigate the rovibrational dynamics of small molecules. Helium nanodroplets are a versatile medium that simplifies the spectroscopy of embedded molecules owing to their low temperature (0.4 K) and weakly interacting nature. In the infrared spectral region, this often results in a small number of rotationally resolved lines that can be observed and analyzed within several lab periods. We demonstrate the advantages of using this well-established technique in an upper-level undergraduate chemistry course for which the laser spectroscopy of helium solvated ¹³C-labelled formic acid was investigated for the first time.

1. Introduction

Studying the medium/high resolution infrared spectroscopy of molecules in the gas phase is a standard physical chemistry experiment that is typically introduced early on in a quantum chemistry laboratory course. For the most part, small linear molecules are investigated, with the most common being HCl [1]; this is on account of its lightness, large transition dipole moment, and putative simplicity (effectively having only one unique rotational constant; inversely proportional to the moment of inertia, I). Typically, the goal of such an experiment is to perform a fit of spectroscopic constants (ground and excited rotational constants, band origin, centrifugal distortion constants) to the line positions, ultimately affording the structural parameters of the investigated molecule, such as the bond length, r (from the relation $I = \mu r^2$). More complicated species with two unique moments of inertia are sometimes investigated by infrared spectroscopy in an undergraduate course, such as CH3I [2]. This naturally requires the inclusion of additional parameters in the fit, such as multiple band origins, rotational constants, and Coriolis coupling constants. The most complicated type of molecule, having three unique moments of inertia is typically avoided in undergraduate spectroscopy laboratories because the infrared spectra can be exceptionally rich, often displaying 1000s of lines at room temperature. It should be noted that in teaching laboratories that are equipped with microwave spectrometers, that it is more feasible for students to investigate asymmetric tops [3-5], especially when the sample is generated in a supersonic expansion (vide infra) [6,7].

The rotationally resolved spectrum of a given molecule can be

simplified by lowering the rotational temperature of the sample. Various techniques can be used for this purpose, for example, buffer gas cooling [8], and cooling in a supersonic expansion [9,10]. These techniques typically result in a reduction in the (rotational) temperature by one to two orders of magnitude, giving rise to simplified spectra that are more feasible for students to perform an in-course analysis on. Such spectra, however, often contain many lines that necessitate a somewhat involved analysis: for example, the 12 K spectrum of formic acid in the C-O stretching band (\sim 50 cm⁻¹ broad) was found to contain \sim 200 lines [11], some of which are finely split due to the asymmetry of the molecule (i.e., "asymmetry splittings"). The rotationally resolved spectra can, however, be simplified even further by reducing the temperature by three orders of magnitude relative to the gas phase; this can be accomplished by embedding the molecule of interest in superfluid helium nanodroplets. Fig. 1 provides a comparison of the simulated infrared spectra in the ν_6 band (C—O stretch) of H¹³COOH in the gas phase (using constants reported in Ref. [12]), and in liquid helium nanodroplets (using constants reported here); note the dramatic simplification of the spectrum.

The first high-resolution investigation of a molecule in superfluid helium nanodroplets was performed on SF₆, for which the infrared spectrum revealed rotationally resolved substructure with an intensity distribution that is consistent with a rotational temperature of \sim 0.4 K [13]. Several years later the infrared helium nanodroplet spectrum of OCS in the C—O stretching fundamental was reported [14], which contains a small number of baseline resolved *P* and *R* branch peaks that can be analyzed using standard linear rotor energy level expressions. A

E-mail address: rastonpl@jmu.edu.

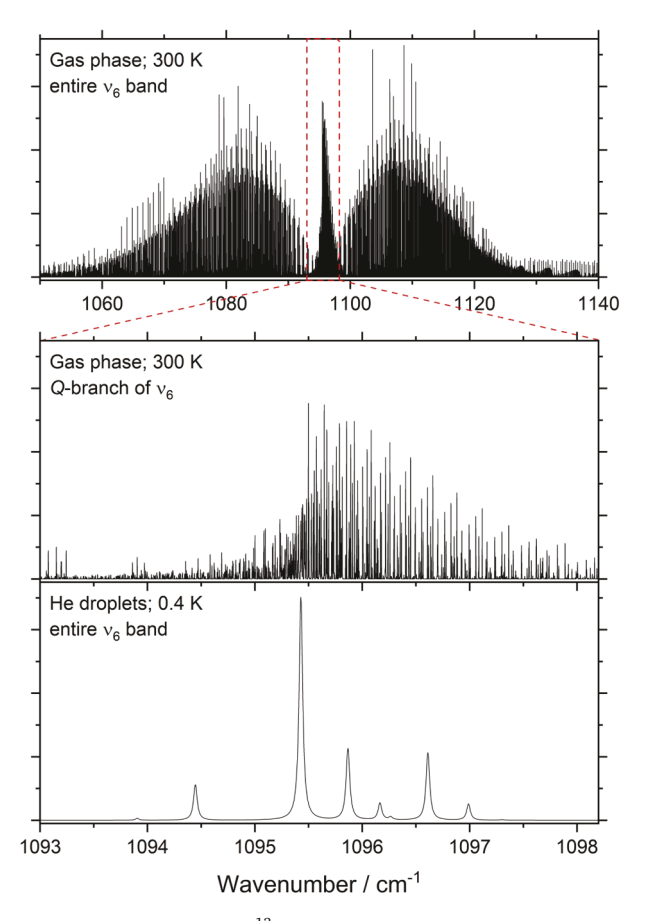


Fig. 1. Simulated spectra of $\rm H^{13}COOH$ at 300 K in the gas phase (Gaussian linewidth of 0.002 cm $^{-1}$, FWHM), and at 0.4 K in liquid helium nanodroplets (Lorentzian linewidth of 0.04 cm $^{-1}$, FWHM).

couple of years later, formic acid was investigated in the vicinity of the O—H and C—H stretching fundamentals [15]. While evidence for extensive Fermi and Coriolis coupling was found (differing linewidths between the bands), the rotational substructure within each band was well resolved, and analysis of the small number of peaks (\leq 6) within each band resulted in determination of the rovibrational parameters (ν_0 , A, B, C). In the following, we describe the value of employing this technique in an undergraduate teaching lab, and show data (and analysis) collected (and performed) by students on formic acid in helium nanodroplets.

2. The experiment

The helium nanodroplet isolation spectrometer the experiments were performed on was mostly built by undergraduate students over the course of \sim 2 years. It has been described in detail elsewhere [16–18], and here we provide only pertinent details; for additional information about the technique please see Refs. [19-28]. Fig. 2 shows the spectrometer, highlighting the three vacuum chambers that are labelled according to their functionality: the "Source Chamber", "Pick-up Chamber", and "Detection Chamber". Helium nanodroplets are produced in the source chamber by expanding high purity (99.9995%) helium gas at a pressure of 34.5 bar through a nozzle (~5 μm) held at \sim 19.5 K. Under these conditions the average droplet size ($\langle N \rangle$) is 2.4 \times 10^3 atoms, which is determined using well established empirical scaling laws that relate it to the backing pressure, nozzle size, and nozzle temperature [29,30]. The expansion is skimmed (0.51 mm dia.) at the end of the source chamber, and the newly formed helium droplet beam passes into the pick-up chamber where it encounters gas phase ¹³C-labelled formic acid. The pressure of the dopant is optimized so that on average,

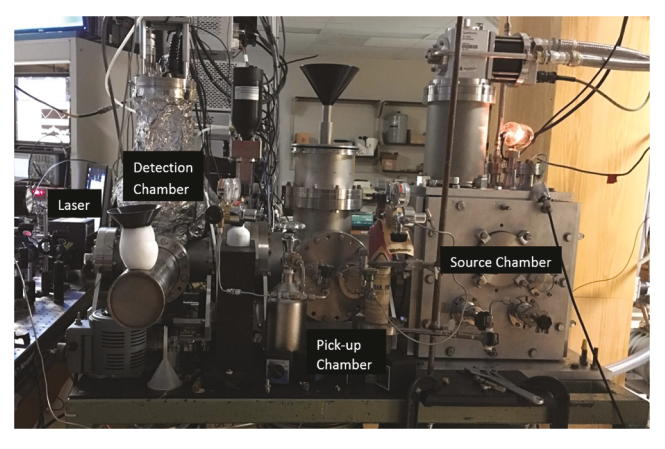


Fig. 2. The JMU helium nanodroplet isolation spectrometer. The source and pick-up chambers are evacuated with diffusion pumps and the detection chamber is evacuated with a turbo pump.

one molecule is picked-up per droplet. The pick-up process involves a room temperature molecule colliding with a helium nanodroplet; the thermal conductivity of superfluid helium is 30x that of copper, and this allows for the excess kinetic energy of the molecule to be rapidly liberated through the evaporation of several hundred helium atoms. The captured molecule at 0.4 K can then be interrogated by laser spectroscopy before entering the detection chamber.

The output of an external cavity quantum cascade laser (\sim 9–10 µm) was aligned antiparallel to the helium nanodroplet beam. The laser beam was chopped and focused to a point somewhere in between pickup and detection, and can be tuned with a modified computer program previously developed [31]. When the laser is resonant with a rovibrational transition of a captured formic acid molecule, it can absorb a photon. In the C—O stretching band investigated here this corresponds to an energy (E_n/hc) of ~1095 cm⁻¹, and since the binding energy of helium is $\sim 5 \text{ cm}^{-1}$ [32], absorption of a photon, followed by vibrational relaxation, will (on paper) result in the evaporation of \sim 220 atoms from the droplet (i.e., $\Delta N = 1095/5$). After the droplet beam is interrogated by the output of the laser, it encounters an off-axis quadrupole mass spectrometer that is housed in the detection chamber. A small fraction of droplets are ionized by electron impact in this chamber, with a probability that is proportional to their geometric cross section (which varies by $N^{2/3}$). Ionization of doped droplets typically gives rise to a positive charge on helium that migrates through the droplet until it encounters the embedded molecule (such as H¹³COOH), and since the ionization potential of any impurity is substantially less than that of helium, droplet explosion and molecular fragmentation typically occurs [33]. The resulting positively charged fragments with masses greater than \sim 6 u are transmitted through the quadrupole mass filter and detected with an electron multiplier tube. The resulting signal is processed with a lockin amplifier with a phase angle optimized such that a positive output signal corresponds to depletion.

3. Instrument preparation and data acquisition

Helium nanodroplet isolation spectrometers consist of a large number of components, some of which are semi-permanently on while others are on for the duration of the experiment. Major equipment that falls into the latter category on the JMU helium nanodroplet isolation spectrometer are the diffusion pumps, closed cycle helium cryostat, and mass spectrometer. Our system is configured such that we can remotely activate these components by way of an email to a Raspberry PiTM. We turn these components on a couple of hours before experimentation, with the cool down of the coldhead taking the longest. Students enter the lab after cool down, and configure the spectrometer for the planned experiment(s). This involves transferring several mL of liquid sample

(for the formic acid experiment) into a round bottom flask with a $1/4^{\prime\prime}$ SS pipe fitting, and coupling that to an inlet flange on the pick-up chamber. A needle valve is used to control the sample flow into the chamber, and after evacuating the head gas, it is adjusted to a pressure of $\sim\!5\times10^{-6}$ torr [34], which is optimized for the pick-up of one molecule per droplet. It is instructive to measure the mass spectrum of the neat droplet beam, and compare it with what is observed after doping the droplets. Before doing this, students fill the liquid nitrogen Dewars (on the pick-up and detection chambers) and open a solenoid driven pneumatic gate valve (8″ CF) that separates the last two chambers.

After establishing that helium droplet conditions are optimized, students turn on "optical" elements, which correspond to the infrared laser, piezo driver, wavemeter, and chopper wheel. Before scanning the laser, the group of students discuss a wavenumber range that would be most efficient to scan based on previous helium nanodroplet investigations (which show that vibrational shifts in going from the gas phase to helium is $\sim 1~\text{cm}^{-1}$), taking into account the band origin, band type, and rotational constants of the target molecule in the gas phase. For H¹³COOH in the C—O stretching band, these are very accurately known [35]. After establishing suitable parameters for collecting the spectrum (scan range, scan speed, data acquisition rate, lock-in sensitivity...), students begin scanning and acquiring data. While we have LabVIEW programs that fully automate the scanning, it is more engaging to manually control the coarse stepping of the laser (while a separate program applies a triangle wave to the piezo element of the laser for the fine scanning). In this way, over the course of about two hours, the data corresponding to the spectrum shown in Fig. 3 was collected (this is after data reduction [31]).

4. Spectroscopic analysis

4.1. Computer assisted fitting

A number of computer programs have been developed that can be utilized for fitting spectroscopic parameters to rotationally resolved spectra [36–42]. Arguably, the most user friendly of these is PGOPHER [40], which makes it well suited for incorporation into undergraduate coursework. The spectrum shown in Fig. 3 was collected by one group of

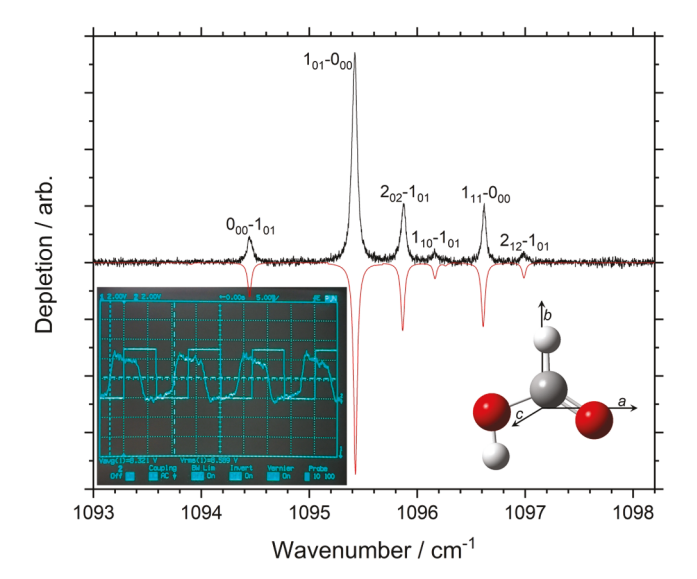


Fig. 3. Experimental (black) and simulated (red) spectra of H¹³COOH in helium nanodroplets in the C—O stretching fundamental. The constants from Table 1 along with a temperature of 0.4 K and Lorentzian linewidth (FWHM) of 0.04 cm⁻¹ was used in the simulation. The right inset shows the principal inertial axes superimposed on the CCSD(T)/aug-cc-pVQZ optimized structure of formic acid, and the left inset shows a typical depletion signal students observe in "real time".

six students who were enrolled in the Biophysical Chemistry course, each of which performed a fit of the spectroscopic parameters to the line positions. Leading into this experiment we had covered rovibrational spectroscopy of nothing more complicated than linear molecules in our guided inquiry Quantum Chemistry & Spectroscopy course (that all six students were enrolled in). Additional background material on asymmetric tops ($I_a \neq I_b \neq I_c$) had to be covered to ensure that the significance of the molecular parameters used in the model were adequately understood. This involved discussing material from Section 6.5 in Ref. [43], which shows how rigid asymmetric rotor energy level expressions can be derived, along with mention of selection rules and line intensities.

Students began by simulating the infrared spectrum of gas phase H¹³COOH with PGOPHER, using the known band origin and principal rotational constants (for the ground and excited C—O stretching states) [35,44], along with a reasonable estimate of the band type (which can be readily done with most electronic structure computational packages). Since the default temperature is 300 K in PGOPHER, 100s of rotational states are populated which gives rise to 1000s of lines in the simulated spectrum [45]. An extended activity on the Boltzmann distribution ("Population of Quantum States" [46]) was covered before fitting the experimental spectrum, which gave students the necessary background on the effect that temperature has on the infrared band profiles (as shown in Fig. 1). Thus, the very dramatic effect that reducing the temperature in the simulation from 300 K to 0.4 K (the temperature of helium droplets) was immediately appreciated. In fact, at this stage the simulated lines could be readily assigned to the observed ones, and the spectroscopic parameters optimized. The result of doing this is shown in Fig. 3, which reveals excellent agreement between the experimental and simulated spectra, the latter of which was generated using the constants listed in Table 1.

4.2. Manual fitting

An alternative method of analyzing the spectrum is to determine the constants by taking the combination differences of transitions. This method requires more of an understanding of asymmetric top molecular energy levels so that assignments can be readily made (see Fig. 3). The first step is to generate a list of line positions, assignments, and energy level expressions [43], similar to what is shown in Table 2, where we labelled each transition with a lowercase italicized letter (for convenience). The logical starting point in analyzing the spectrum shown in Fig. 3 seems to lie in taking the difference between transition f and e, which is equal to 4C'. Next, A' can be determined by realizing it's equal to [-a+c-d+e]/2, and similarly, B' is equal to [a-c-d+e]/2. The band origin can then be determined by subtracting the appropriate (just determined) upper state rotational constants from either transition a or c. Finally, B''+C'' is most easily gotten by subtracting d from the band origin. It is satisfying and instructive to perform a check to see if the constants are correct by calculating the line position of transition *b* (the only one not included in the analysis) using the determined spectroscopic constants.

Table 1Spectroscopic parameters of H¹³COOH embedded in helium nanodroplets; uncertainties (in last place) are estimated. Values were determined by students in a Biophysical Chemistry course using PGOPHER.

	ν_o	Α'	В'	C'	(B''+C'')/2
Gas ^a	1095.403646	2.522449	0.40012796	0.34396941	0.37413491
He	1094.954(2)	1.451(2)	0.268(1)	0.206(1)	0.254(1)
Gas/ He	1.000411	1.739	1.492	1.668	1.473

^a From Ref. [12].

Table 2Lines positions and assignments for H¹³COOH embedded in helium nanodroplets. Also included are the rigid asymmetric rotor energy level expressions for the ground (") and excited (') states.

$J'_{Ka'Kc'}$ - $J''_{Ka''Kc''}$	$v (\text{cm}^{-1})$	F'	F"	label
1 ₀₁ -0 ₀₀	1095.420	<i>B</i> '+ <i>C</i> '	0	а
$2_{02} - 1_{01}$	1095.873	$2A'+2B'+2C'-2((B'-C')^2+(A'-C')(A'-B'))^{1/2}$	B''+C''	b
1 ₁₁ -0 ₀₀	1096.620	A'+C'	0	с
$0_{00} - 1_{01}$	1094.449	0	B''+C''	d
1_{10} -1_{01}	1096.161	A'+B'	B''+C''	e
$2_{12} - 1_{01}$	1096.985	A'+B'+4C'	B''+C''	f

Table 3 Moments of inertia from the helium nanodroplet experiment on $\rm H^{13}COOH$ (values for the excited vibrational state). Units are amu*Å².

	He + rotor	Rotor ^a	Не
I_a	11.6	6.68	4.93
I_b	62.9	42.1	20.8
I_c	81.8	49.0	32.8

a From Ref. [12].

4.3. Hybrid approach

What we label as the "hybrid approach" involves determining the entries in Table 2 (which entails assigning peaks and determining term values), then performing a least-squares fit. While a number of different programming languages can be used for this purpose (e.g., FORTRAN, C++, Mathematica...), we opted for Python (with the NumPy and SciPy extension modules). The code that was written (21 lines) could be developed by undergraduate students with little programming experience in the time taken to average the spectra (\sim 2 h). It returns the same constants as did PGOPHER (see Table 1).

5. Inertial analysis

Following the spectroscopic analysis, an inertial analysis allows for a closer connection to be made with the physical attributes of the system. The moment of inertia about a certain axis is obtained by inverting the corresponding rotational constant, e.g., $I_a = \frac{h}{8 \, \pi^2 \, c \, m_u \, A}$ where I_a is the moment of inertia about the a-axis (in amu·m²), h is Planck's constant (in J·s), m_u is the atomic mass constant (in kg/amu), c is the speed of light (in cm/s), and A is the rotational constant about the a-axis (in cm⁻¹). A convenient conversion ratio (if pressed for time) is $I_a = (16.8576 \cdot \text{amu·Å}^2 \cdot \text{cm}^{-1})/A$. In this way the moments of inertia about the three principal inertial axes for H¹³COOH were obtained, both in the gas phase and in superfluid helium nanodroplets (see Table 3).

By taking the difference between the gas phase and helium solvated moments of inertia, one obtains the moment of inertia of helium ($\Delta I_{\rm He}$) that couples to the molecule as it rotates about each of the principal axes. What the students found for this molecule is that the amount of helium that couples to rotation decreases with increasing angular velocity (which is proportional to the rotational constant; see Table 3): as noted by one team of students, "The moment of inertia for helium about the a-axis may be concerningly low, however, since the rotational constant is so high for the a-axis, it may be explained that since formic acid is rotating so fast, it may not drag as much helium along for the ride". This is known as breakdown of the adiabatic following approximation, and reference to the literature on this aspect of the investigation can be made [16,17,47,48].

6. Summary & outlook

Here we highlighted the value of including the technique of helium

nanodroplet isolation spectroscopy in a teaching laboratory by way of an example molecule that was explored by undergraduate students. The molecule chosen was $\mathrm{H}^{13}\mathrm{COOH}$ because it is biophysically relevant, it has a large C—O stretching transition moment, it is relatively small (which allows for rotationally resolved peaks), and most importantly it is accessible with our (borrowed) laser system. This investigation was performed after acquiring and analyzing the gas phase infrared spectra of the linear rotors, CO and CO_2 (formed from the pyrolysis of formic acid), in addition to covering basic molecular spectroscopy in an activity-based Quantum Chemistry & Spectroscopy course. The primary learning outcome was that students got to advance their understanding of rovibrational spectroscopy by investigating an asymmetric rotor, and in doing so they utilized state-of-the-art instrumentation that is uncommonly included in undergraduate courses.

It is important to note that while the normal isotopologue of formic acid has previously been explored in helium nanodroplets (as has the monodeuterated form) [15,49], this is the first time that 13 C-labelled formic acid has been investigated. Part of the motivation in doing so was to provide a mini course-based undergraduate research experience (CURE) [50], with the hopes of recruiting student(s) to continue the research project after completion of the course it was seeded in. Future research directions include investigating the infrared spectra of formic acid clusters, beyond the dimer [51], and to this end a spectrum has been collected in-lab with preliminary assignments made.

In closing, we note that there are many potentially interesting unexplored molecules that can be investigated by helium nanodroplet isolation spectroscopy, and a relatively simple one we plan to investigate in Physical Chemistry II Lab is methyl fluoride (CH₃F), since it is small, and it has a very bright C-F stretching vibration that falls within the tuning range of our current laser system. Additionally, as noted by Craig and Lacuesta [52], the laboratory-based infrared investigation of a molecule with different symmetry species will provide students with a somewhat rare opportunity to consolidate the group theory they may have learnt in inorganic or physical chemistry courses.

CRediT authorship contribution statement

Paul L. Raston: Conceptualization, Writing - review & editing.

Declaration of Competing Interest

The authors declare that they have no known competing financial interests or personal relationships that could have appeared to influence the work reported in this paper.

Acknowledgements

This work was supported by the Research Corporation for Science Advancement (Cottrell Scholar Award), and the National Science Foundation (CAREER Award No. CHE-2141774). We would like to express our appreciation to G. E. Douberly for the loan of the laser used by the students in this work. We are grateful to C. Tanjaroon for technical assistance, T. Faulkner and I. Miller for building/automating the

spectrometer, and to the "The Biophys Gang" (class of 2020; P. Alvarado, S. Clark, C. Dodd, M. Gamboa, J. Skubal, and J. White) who carried out the helium nanodroplet investigation featured here. Finally, we wish to acknowledge the late Norman C. Craig, whose vast body of work that features the efforts of many undergraduate students, is inspirational.

References

- [1] F.E. Stafford, C.W. Holt, G.L. Paulson, J. Chem. Ed. 40 (1963) 245.
- [2] I.J. McNaught, J. Chem. Ed. 59 (1982) 879.
- [3] S.G. Kukolich, Am. J. Phys. 41 (1973) 1084.
- [4] R.H. Schwendeman, H.N. Volltrauer, V.W. Laurie, E.C. Thomas, J. Chem. Ed. 47 (1970) 526.
- [5] J.L. Hollenberg, J. Chem. Ed. 47 (1970) 2.
- [6] A. Duerden, N. Moon, G.S. Grubbs, J. Chem. Ed. 98 (2021) 1008.
- [7] S.A. Cooke, P. Ohring, J. Spectrosc. 2013 (2013) 698392.
- [8] J.K. Messer, F.C. De Lucia, Phys. Rev. Lett. 53 (1984) 2555.
- [9] R.E. Smalley, B.L. Ramakrishna, D.H. Levy, L. Wharton, J. Chem. Phys. 61 (1974) 4363.
- [10] A.R. Skinner, D.W. Chandler, Am. J. Phys. 48 (1980) 8.
- [11] K.G. Goroya, Y. Zhu, P. Sun, C. Duan, J. Chem. Phys. 140 (2014) 164311.
- [12] O. Baskakov, V.M. Horneman, S. Alanko, J. Lohilahti, J. Mol. Spec. 249 (2008) 60.
- [13] M. Hartmann, R.E. Miller, J.P. Toennies, A. Vilesov, Phys. Rev. Lett. 75 (1995) 1566.
- [14] S. Grebenev, M. Hartmann, M. Havenith, B. Sartakov, J.P. Toennies, A.F. Vilesov, J. Chem. Phys. 112 (2000) 4485.
- [15] F. Madeja, P. Markwick, M. Havenith, K. Nauta, R.E. Miller, J. Chem. Phys. 116 (2002) 2870.
- [16] T. Faulkner, I. Miller, P.L. Raston, J. Chem. Phys. 148 (2018) 044308.
- [17] I. Miller, T. Faulkner, P.L. Raston, J. Phys. Chem. A 123 (2019) 1630.
- [18] I. Miller, T. Faulkner, J. Saunier, P.L. Raston, J. Chem. Phys. 152 (2020) 221102.
- [19] J.P. Toennies, A.F. Vilesov, Annu. Rev. Phys. Chem. 49 (1998) 1.
- [20] C. Callegari, K.K. Lehmann, R. Schmied, G. Scoles, J. Chem. Phys. 115 (2001) 10090.
- [21] J.P. Toennies, A.F. Vilesov, Angew. Chem.-Int. Edit. 43 (2004) 2622.
- [22] M.Y. Choi, G.E. Douberly, T.M. Falconer, W.K. Lewis, C.M. Lindsay, J.M. Merritt, P. L. Stiles, R.E. Miller, Int. Rev. Phys. Chem. 25 (2006) 15.
- [23] F. Stienkemeier, K.K. Lehmann, J. Phys. B 39 (2006) R127.
- [24] J. Kupper, J.M. Merritt, Int. Rev. Phys. Chem. 26 (2007) 249.
- [25] K. Szalewicz, Int. Rev. Phys. Chem. 27 (2008) 273.

- [26] S. Yang, A.M. Ellis, Chem. Soc. Rev. 42 (2013) 472.
- [27] D. Verma, R.M.P. Tanyag, S.M.O. O'Connell, A.F. Vilesov, Adv. Phys.: X 4 (2019).
- [28] P.L. Raston, Phys. Chem. Chem. Phys. 23 (2021) 25467.
- [29] E. Knuth, B. Schilling, J.P. Toennies. Proceedings of the 19th International Symposium on Rarefied Gas Dynamics, Oxford University Press, London, 1995.
- [30] P.L. Raston, SoftwareX 14 (2021) 100703.
- [31] A.M. Morrison, T. Liang, G.E. Douberly, Rev. Sci. Inst. 84 (2013) 013102.
- [32] V.R. Pandharipande, J.G. Zabolitzky, S.C. Pieper, R.B. Wiringa, U. Helmbrecht, Phys. Rev. Lett. 50 (1983) 1676.
- [33] W.K. Lewis, B.E. Applegate, J. Sztáray, B. Sztáray, T. Baer, R.J. Bemish, R.E. Miller, J. Am. Chem. Soc. 126 (2004) 11283.
- [34] We note this is the raw (uncorrected) ion gauge reading.
- [35] P.P. Ong, K.L. Goh, H.H. Teo, J. Mol. Spec. 194 (1999) 203.
- [36] H.M. Pickett, J. Mol. Spec. 148 (1991) 371.
- [37] N. Tasinato, A.P. Charmet, P. Stoppa, J. Mol. Spec. 243 (2007) 148.
- [38] N.A. Seifert, I.A. Finneran, C. Perez, D.P. Zaleski, J.L. Neill, A.L. Steber, R. D. Suenram, A. Lesarri, S.T. Shipman, B.H. Pate, J. Mol. Spec. 312 (2015) 13.
- [39] D. Licari, N. Tasinato, L. Spada, C. Puzzarini, V. Barone, J. Chem. Theory Comput. 13 (2017) 4382.
- [40] C.M. Western, J. Quant. Spectrosc. Radiat. Transf. 186 (2017) 221.
- [41] D.P. Zaleski, K. Prozument, J. Chem. Phys. 149 (2018).
- [42] C.M. Western, B.E. Billinghurst, Phys. Chem. Chem. Phys. 21 (2019) 13986.
- [43] P.F. Bernath, Spectra of Atoms and Molecules, Oxford University Press, 2005.
- [44] E. Willemot, D. Dangoisse, N. Monnanteuil, J. Bellet, J. Phys. Chem. Ref. Data 9 (1980) 59.
- [45] An interesting extension of this undergraduate laboratory investigation would be to record the gas phase spectrum of H¹³COOH and then simulate and possible fit it, with the inclusion of higher order [centrifugal distortion and Coriolis coupling (!)] constants.
- [46] T.D. Shepherd, A. Grushow, Quantum Chemistry and Spectroscopy: A Guided Inquiry, Wiley, 2014.
- [47] A. Conjusteau, C. Callegari, I. Reinhard, K.K. Lehmann, G. Scoles, J. Chem. Phys. 113 (2000) 4840.
- [48] H. Hoshina, D. Skvortsov, B.G. Sartakov, A.F. Vilesov, J. Chem. Phys. 132 (2010) 074302.
- [49] P. Das, C.J. Knapp, W. Jäger, J. Mol. Spec. 341 (2017) 17.
- [50] https://serc.carleton.edu/curenet/institutes/misc/examples/221478.html (accessed July 2022).
- [51] F. Madeja, M. Havenith, K. Nauta, R.E. Miller, J. Chocholoušová, P. Hobza, J. Chem. Phys. 120 (2004) 10554.
- [52] N.C. Craig, N.N. Lacuesta, J. Chem. Ed. 81 (2004) 1199.